

# Water Ordering at Membrane Interfaces Controls Fusion Dynamics

Peter M. Kasson,<sup>†</sup> Erik Lindahl,<sup>‡,§</sup> and Vijay S. Pande<sup>\*,†,⊥</sup>

<sup>†</sup>Department of Molecular Physiology and Biological Physics, University of Virginia, Charlottesville, Virginia 22903, United States

<sup>‡</sup>Department of Theoretical Physics, Royal Institute of Technology, SE-100 44 Stockholm, Sweden

<sup>§</sup>Center for Biomembrane Research, Stockholm University, SE-106 91 Stockholm, Sweden

<sup>⊥</sup>Department of Chemistry, Stanford University, Stanford, California 94305, United States

**S** Supporting Information

**ABSTRACT:** Membrane interfaces are critical to many cellular functions, yet the vast array of molecular components involved make the fundamental physics of interaction difficult to define. Water has been shown to play an important role in the dynamics of small biological systems, for example when trapped in hydrophobic regions, but the molecular details of water have generally been thought dispensable when considering large membrane interfaces. Nevertheless, spectroscopic data indicate that water has distinct, ordered behavior near membrane surfaces. While coarse-grained simulations have achieved success recently in aiding understanding the dynamics of membrane assemblies, it is natural to ask, *does the missing chemical nature of water play an important role?* We have therefore performed atomic-resolution simulations of vesicle fusion to understand the role of chemical detail, particularly the molecular structure of water, in membrane fusion and at membrane interfaces more generally. These membrane interfaces present a form of *hydrophilic* confinement, yielding surprising, non-bulk-like water behavior.

Water has been shown to play an important role in the dynamics of small biological systems, for example when trapped in hydrophobic regions,<sup>1–5</sup> but the molecular details of water have generally been thought dispensable when considering large membrane interfaces. Nevertheless, spectroscopic data indicate that water has distinct, ordered behavior near membrane surfaces.<sup>6–8</sup> While coarse-grained simulations have achieved success recently in aiding understanding the dynamics of membrane assemblies,<sup>9–11</sup> it is natural to ask, *does the missing chemical nature of water play an important role?* Here, we use atomic-resolution molecular dynamics simulations of membrane fusion to show that water confined between membrane interfaces differs substantially from bulk solvent. More importantly, it has implications for biological function, as the dynamics of this interfacial water help determine the free energy barrier for stalk formation. Our results suggest a dual role for water, where the interfacial water layer speeds fusion overall but slows the final rearrangements, leading to stalk formation. These results illustrate how molecular details of membrane–water interfaces control large-scale outcomes and suggest a way for theory to quantitatively predict free-energy barriers to fusion by drawing on both

membrane mechanics and the physical chemistry of interfacial solvation.

We simulated the fusion of small, 15-nm lipid vesicles connected by an amide cross-linker. In our simulations, vesicle pairs that fuse adhere to form a metastable membrane interface prior to stalk formation and fusion.<sup>12</sup> We have previously suggested that formation of this contact patch helps to accelerate stalk formation.<sup>12</sup> A thin layer of water is present between the vesicles in this contact patch, and this interfacial water shows substantial ordering, differing substantially in its dynamics from bulk water. We assess deviation from bulk-like behavior using a series of molecular-level metrics that have been employed previously:<sup>3,13</sup> water mobility, hydrogen bond dynamics, and rotational entropy.

Initial fusion simulations were performed as previously described:<sup>12</sup> each 15-nm vesicle was composed of 877 POPC or POPE phospholipids using the Berger simulation parameters.<sup>14</sup> The cross-linker structure was  $-\text{CO}(\text{CH}_2)_4\text{CO}-$ , connected to POPC lipids via an amide linkage to the headgroup nitrogen. Individual vesicles were first equilibrated in the TIP3P explicit solvent model of water.<sup>15</sup> Pairs of vesicles were then placed at 1-nm separation in a hexagonal box with sides 21 nm and height 32.5 nm and solvated in TIP3P water, leading to a system size of over a million atoms. Simulations were run using Gromacs 4.0<sup>16</sup> under constant temperature and pressure using Berendsen pressure coupling and the velocity-rescaling thermostat at 310 K.<sup>17</sup> All covalent bond lengths were constrained using LINCS,<sup>18</sup> and long-range electrostatics were computed every step using Particle Mesh Ewald (PME).<sup>19</sup> The amine hydrogen atoms on POPE were converted to virtual interaction sites<sup>16</sup> to enable longer time steps by constraining the internal geometry of the only polar hydrogens in the lipid system. The atomic coordinates are constructed every step, and forces acting on them are interpolated back onto the mass centers. This approach has been shown to conserve energy,<sup>20</sup> but we also checked the model by testing both 2 and 4 fs time steps, with equivalent results for a pair of full fusion trajectories.

As the vesicles approach and make contact, the translational mobility of the water in the interfacial layer drops markedly (Figure 1); the mean 1-ns displacement of water within a 2-nm radius of the interface drops from 5.2 to 1.9 nm. Water molecules in the interfacial layer also have substantially longer hydrogen bond lifetimes (Figure S1), which indicates a more fundamental change than merely forming a two-dimensional water system

**Received:** January 12, 2011

**Published:** February 25, 2011

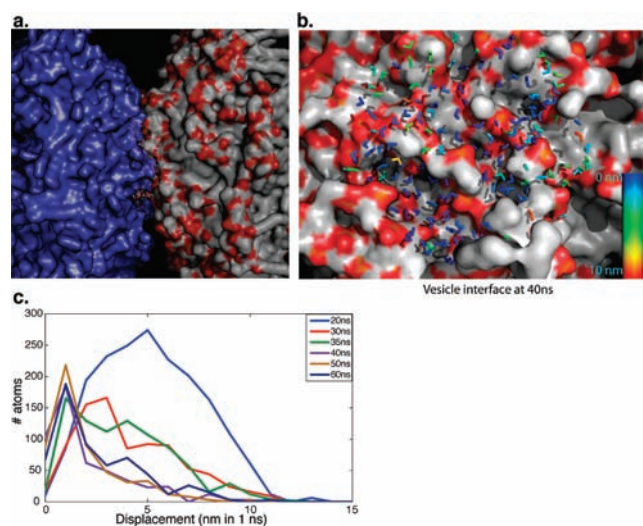


**Figure 1.** Formation of a vesicle–vesicle interface with decreased water mobility. (a) Interface between the vesicles. (b) Distribution of water mobilities at 40 ns, with water molecules rendered in stick form against the surface of one vesicle, colored by displacement within a 1-ns interval. Mobility is greatly slowed compared to a 30-ns snapshot (see Figure S3). (c) Water mobility histograms plotted at different time points as the interface forms. At 20 ns of simulation, there is a broad distribution of water mobilities. By 40 ns, the mobility has dropped sharply, with most water molecules showing a displacement of  $\leq 2$  nm.

with the same dynamics as bulk. This decreased mobility would also explain the finding of anomalously high electrical resistance in the water layer between adherent cells and silica supports,<sup>21</sup> which could result from solvent ordering. In our simulations, the hydrogen bond autocorrelation function exhibits stretched exponential dynamics,  $C(t) = \exp[-(t/\tau)^\beta]$ , for which comparable correlation times can be calculated<sup>22</sup> as  $\tau' = 2^{(1-\beta)/\beta} \tau/\beta \Gamma(1/\beta)$ . Near the vesicle surface, the decay of the hydrogen bond time autocorrelation function is 3-fold slower than in bulk solvent (1 ps vs 0.3 ps), consistent with experimental measurements in reverse micelles<sup>23</sup> and simulations of planar bilayers.<sup>24</sup> This effect is dramatically amplified at the vesicle–vesicle interface. For this interface, the water dynamics is 15-fold slower than on the rest of the vesicle surface and 40-fold slower (12 ps) than in bulk solvent. This slowed rearrangement of interfacial water is analogous to that seen at hydrophobic surfaces and hydrophilic-functionalized surfaces.<sup>25</sup>

The interfacial water layer also displayed reduced rotational entropy (Figure S2). This quantity was measured directly by binning water orientations on a cubic grid and calculating  $S(X) = -\sum P(i,X) \log P(i,X)$ , where  $P(i,X)$  is the probability of a water molecule in voxel  $X$  being assigned to orientational bin  $i$ . A slice through the interface is shown in Figure 2, demonstrating a significant ( $p < 10^{-5}$ ) decrease in rotational entropy near the interface center:  $32.8 \text{ k}_B/\text{nm}^2$  of interfacial area less than bulk for water within 2 nm of the center, and  $66.6 \text{ k}_B/\text{nm}^2$  less than bulk for water within 1 nm.

On the basis of these slowed water dynamics and the strong correlation between patch formation and fusion in our simulations, we hypothesize that this layer of interfacial water plays an important role in stabilizing vesicle contact prior to fusion stalk formation. What, then, is the functional consequence for fusion: do the slow dynamics then promote or hinder stalk formation?

To test this, we compared committor values between our original system and one where the solvent conformations were

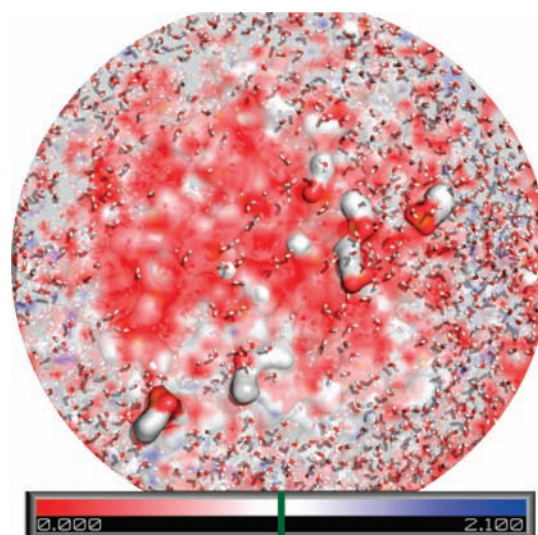


**Figure 2.** Reduced water rotational entropy at the vesicle–vesicle interface. A slice through the vesicle–vesicle interface is plotted, with a colored plane showing water rotational entropy in units of  $k_B$ , colored from red (ordered) to blue (disordered). Entropy was calculated for the 5-ns time interval corresponding to 55–60 ns of the fusion simulation; for reference, a structural snapshot at 55 ns is included. Lipids of the opposing vesicle are shown in surface form and water in stick form. The deep red in the center of the interface denotes a significant decrease in water rotational entropy compared to bulk ( $P < 10^{-5}$ ). A white color (and the green line on the color scale) corresponds to the average rotational entropy of bulk water in our simulation. See Figure S4 for further analysis of the patchy water structure.

resampled at each time point to remove the water “structural memory” (Figure 3). For any reaction  $A \leftrightarrow B$ , committor values<sup>26</sup> measure the fraction of trajectories from a particular starting conformation that reach B before A and thus provide an unbiased estimate of reaction coordinate. Shifts in committor values can be interpreted as changes in the free-energy barrier between A and B.<sup>27</sup>

Committor analysis was performed as follows: shooting trajectories were run by taking snapshots at 5-ns intervals from an original fusion trajectory, randomizing velocities, and running 20–30 new trajectories of at least 20 ns and as much as 128 ns each from each snapshot selected. Each trajectory was assigned to “stalk-committed” if the vesicle pair reached the fusion stalk state before separating, “patch-committed” if the vesicle pair separated before forming a stalk, or “uncommitted” if the trajectory ended before either commitment event occurred. Commitment to the fusion stalk was defined as the presence of at least two lipid tails in every axial slice through the vesicle–vesicle interface; this criterion was identical to commitment to contents mixing in a test subset of simulations where very long trajectories were computed. Separation of vesicles was defined as a distance of  $>7 \text{ \AA}$  between the closest lipid tails from opposing vesicles.

Solvent resampling was performed by resolving the system from a water bath with the vesicles held fixed and then continuing the simulation. The resolution procedure at each committor snapshot involved removing all water from the snapshot structure, replacing it with water from an equilibrated box, and relaxing the water for 10 ps of simulation with the lipids position-restrained using a spring constant of  $1000 \text{ kJ mol}^{-1} \text{ nm}^{-2}$  in each of the  $x$ ,  $y$ , and  $z$  directions.

Once a contact patch has been formed between vesicles, resolution speeds the fusion process significantly (Figure 3) and

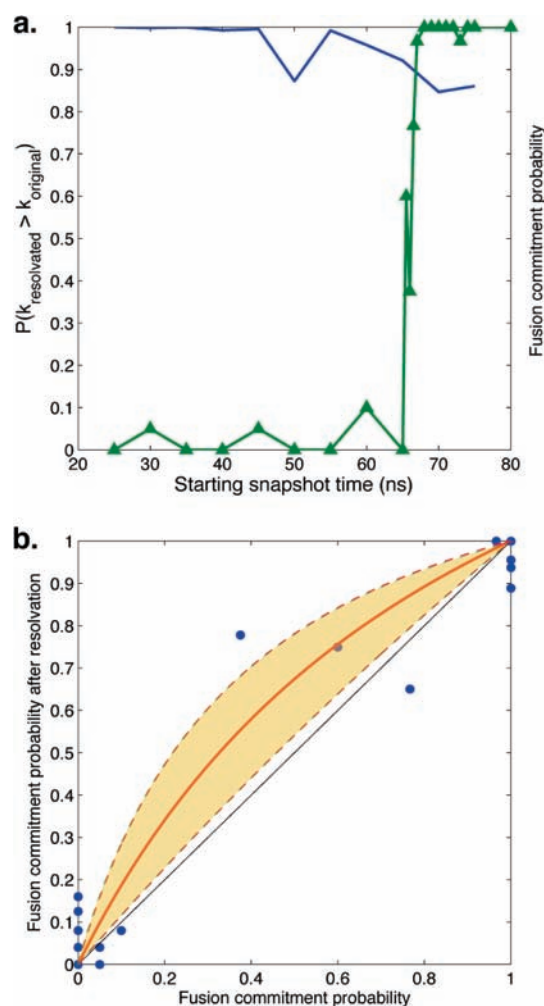


**Figure 3.** Resampling water conformations reduces the barrier to fusion. (a) Probability that resampling water conformations speeds fusion stalk formation for each snapshot examined, plotted in blue. Acceleration probability was calculated using a single-barrier approximation as described previously.<sup>30</sup> For reference, the stalk commitment probability of the original system is plotted in green. The transit time from <20% to >90% commitment probability is less than 5 ns (occurring between 65 and 70 ns of the original simulation). (b) Stalk commitment probabilities plotted with and without resampling water conformations; the data are fit to a free-energy barrier shift formula as per ref 31. The red line shows the maximum-likelihood fit ( $\Delta\Delta G = 0.72 k_B T$ ), with dotted lines and the shaded region between giving 5% and 95% confidence bounds via bootstrap resampling. For reference, a hypothetical  $\Delta\Delta G$  of 0 is plotted in black.

produces a modest shift in committor values, corresponding to a reduction in the free-energy barrier to stalk formation. Hence, there is a marked dynamic effect and a small but significant thermodynamic effect.

These findings suggest that the interfacial water layer stabilizes contact between vesicles, providing greater surface area and prolonged time for lipid tails to encounter each other and form a fusion stalk. However, the same slowed dynamics also makes it harder to finally break the interfacial layer and thus forms a major part of the free-energy barrier to fusion from this contact state. We thus propose a “hurry up and wait” model for the role of interfacial water in fusion, where the water speeds the overall fusion process but paradoxically slows the final rearrangements for stalk formation.

This solvent ordering at the vesicle–vesicle interface differs from hydrophobic dewetting in that no liquid–vapor interface is formed and the mean number of hydrogen bonds per water molecule does not decrease upon interface formation (there is a slight but not statistically significant increase; see Figure S5). However, membrane interfaces and hydrophobic dewetting have an important common theme: non-bulk-like molecular properties of water are key to understanding complex biological behavior. Indeed, the interfacial water forms extensive hydrogen bonds with the polar lipid head groups, and the increase in hydrogen bond order involves both water–water and water–headgroup bonds.

Our results show not only that water between two membranes has altered dynamics, but also that the conformational state of this water can control the fusion reaction between the two membranes. In this case, water acts like molecular flypaper, helping the vesicles stick to each other but slowing rearrangements at the interface that are necessary for fusion. Cellular adhesion to synthetic surfaces and other cells also involves patches of close membrane contact;<sup>21,28,29</sup> we propose that water in these interfacial layers will display similar properties. As simulation and high-resolution experimental techniques are better able to measure dynamics at membrane interfaces, the importance of the hitherto underappreciated molecular nature of water may thus be realized in large biological systems as well as small molecular interfaces.

## ■ ASSOCIATED CONTENT

**S Supporting Information.** Additional analyses, including Figures S1–S5. This material is available free of charge via the Internet at <http://pubs.acs.org>.

## ■ AUTHOR INFORMATION

### Corresponding Author

pande@stanford.edu

## ■ ACKNOWLEDGMENT

The authors thank L. Maibaum, S. Pronk, and C. Stroupe for helpful discussions. P.M.K. was supported by a grant from Stockholm Center for Biomembrane Research and the Foundation for Strategic Research, and E.L. was supported by ERC 209825. Computational resources were provided by SNIC 014/10-31, NSF CBET-0960306, and Folding@Home donors worldwide.

## ■ REFERENCES

- (1) Chandler, D. *Nature* **2005**, *437*, 640–647.
- (2) Berne, B. J.; Weeks, J. D.; Zhou, R. *Annu. Rev. Phys. Chem.* **2009**, *60*, 85–103.
- (3) Liu, P.; Huang, X.; Zhou, R.; Berne, B. J. *Nature* **2005**, *437*, 159–162.
- (4) Mittal, J.; Hummer, G. *Proc. Natl. Acad. Sci. U.S.A.* **2008**, *105*, 20130–20135.
- (5) Giovambattista, N.; Lopez, C. F.; Rossky, P. J.; Debenedetti, P. G. *Proc. Natl. Acad. Sci. U.S.A.* **2008**, *105*, 2274–2279.
- (6) Cheng, J. X.; Pautot, S.; Weitz, D. A.; Xie, X. S. *Proc. Natl. Acad. Sci. U.S.A.* **2003**, *100*, 9826–9830.
- (7) Higgins, M. J.; Polcik, M.; Fukuma, T.; Sader, J. E.; Nakayama, Y.; Jarvis, S. P. *Biophys. J.* **2006**, *91*, 2532–2542.
- (8) Fukuma, T.; Higgins, M. J.; Jarvis, S. P. *Biophys. J.* **2007**, *92*, 3603–3609.

- (9) Reynwar, B. J.; Illya, G.; Harmandaris, V. A.; Muller, M. M.; Kremer, K.; Deserno, M. *Nature* **2007**, *447*, 461–464.
- (10) Marrink, S. J.; de Vries, A. H.; Mark, A. E. *J. Phys. Chem. B* **2004**, *108*, 750–760.
- (11) Shillcock, J. C.; Lipowsky, R. *Nat. Mater.* **2005**, *4*, 225–228.
- (12) Kasson, P. M.; Lindahl, E.; Pande, V. S. *PLoS Comput. Biol.* **2010**, *6*, e1000829.
- (13) Lucent, D.; Snow, C. D.; Aitken, C. E.; Pande, V. S. *PLoS Comput. Biol.* **2010**, *6*, e1000963.
- (14) Berger, O.; Edholm, O.; Jahnig, F. *Biophys. J.* **1997**, *72*, 2002–2013.
- (15) Jorgensen, W. L.; Chandrasekhar, J.; Madura, J. D.; Impey, R. W.; Klein, M. L. *J. Chem. Phys.* **1983**, *79*, 926–935.
- (16) Hess, B.; Kutzner, C.; van der Spoel, D.; Lindahl, E. *J. Chem. Theory Comput.* **2008**, *4*, 435–447.
- (17) Bussi, G.; Donadio, D.; Parrinello, M. *J. Chem. Phys.* **2007**, *126*, 014101.
- (18) Hess, B. *J. Chem. Theory Comput.* **2008**, *4*, 116–122.
- (19) Darden, T.; York, D.; Pedersen, L. *J. Chem. Phys.* **1993**, *98*, 10089–10092.
- (20) Bjellmar, P.; Larsson, P.; Cuendet, M. A.; Hess, B.; Lindahl, E. *J. Chem. Theory Comput.* **2010**, *6*, 459–466.
- (21) Kiessling, V.; Muller, B.; Fromherz, P. *Langmuir* **2000**, *16*, 3517–3521.
- (22) Brandt, E. G.; Edholm, O. *J. Chem. Phys.* **2010**, *133*, 115101.
- (23) Moilanen, D. E.; Fenn, E. E.; Wong, D.; Fayer, M. D. *J. Am. Chem. Soc.* **2009**, *131*, 8318–8328.
- (24) Bhide, S. Y.; Berkowitz, M. L. *J. Chem. Phys.* **2006**, *125*, 094713.
- (25) Li, J.; Liu, T.; Li, X.; Ye, L.; Chen, H.; Fang, H.; Wu, Z.; Zhou, R. *J. Phys. Chem. B* **2005**, *109*, 13639–13648.
- (26) Du, R.; Pande, V. S.; Grosberg, A. Y.; Tanaka, T.; Shakhnovich, E. S. *J. Chem. Phys.* **1998**, *108*, 334–350.
- (27) Rhee, Y. M.; Pande, V. S. *J. Phys. Chem. B* **2005**, *109*, 6780–6786.
- (28) Braun, D.; Fromherz, P. *Appl. Phys. a—Mater.* **1997**, *65*, 341–348.
- (29) Wrobel, G.; Holler, M.; Ingebrandt, S.; Dieluweit, S.; Sommerhage, F.; Bochem, H. P.; Offenhausser, A. *J. R. Soc. Interface* **2008**, *5*, 213–222.
- (30) Kasson, P. M.; Ensign, D. L.; Pande, V. S. *J. Am. Chem. Soc.* **2009**, *131*, 1338–1340.
- (31) Lucent, D.; Vishal, V.; Pande, V. S. *Proc. Natl. Acad. Sci. U.S.A.* **2007**, *104*, 10430–10434.